The Astrophysical Journal, 659:L65–L68, 2007 April 10

TEMPERATURE ANISOTROPY IN A SHOCKED PLASMA: MIRROR-MODE INSTABILITIES IN THE HELIOSHEATH

Y. Liu,[1,2] J. D. Richardson,[1,2] J. W. Belcher,[1] and J. C. Kasper[1]

Received 2007 January 19; accepted 2007 February 21; published 2007 March 2

ABSTRACT

We show that temperature anisotropies induced at a shock can account for interplanetary and planetary bow shock observations. Shocked plasma with enhanced plasma β is preferentially unstable to the mirror-mode instability downstream of a quasi-perpendicular shock and to the fire-hose instability downstream of a quasi-parallel shock, consistent with magnetic fluctuations observed downstream of a large variety of shocks. Our theoretical analysis of the solar wind termination shock suggests that the magnetic holes observed by *Voyager 1* in the heliosheath are produced by the mirror-mode instability. The results are also of astrophysical interest, providing an energy source for plasma heating.

Subject headings: instabilities — shock waves — solar wind

Online material: color figures

1. INTRODUCTION

Planetary bow shocks and interplanetary shocks serve as a unique laboratory for the study of shock waves in collisionless plasmas. Observations of these shocks usually show that ion distributions are anisotropic with respect to the background magnetic field downstream of the shocks. Mirror-mode waves associated with this anisotropy are observed downstream of quasi-perpendicular shocks (defined by the angle between the shock normal and the upstream magnetic field $\theta_{Bn} > 45°$) when the plasma β is high ($\beta > 1$; Kaufmann et al. 1970; Tsurutani et al. 1992; Violante et al. 1995; Bavassano Cattaneo et al. 1998; Liu et al. 2006b). Mirror-mode waves do not grow in low-β regions where the ion-cyclotron mode dominates (e.g., Anderson et al. 1994; Czaykowska et al. 2001). Magnetic fluctuations downstream of quasi-parallel shocks ($\theta_{Bn} < 45°$) have not been identified in detail, but hybrid simulations show that the fire-hose instability can occur downstream of these shocks for certain ranges of upstream Alfvén Mach numbers (M_A) and plasma β's (for instance, $M_A \geq 3$ at $\beta \sim 0.5$; Kan & Swift 1983; Krauss-Varban & Omidi 1991); observations seem to confirm this point (e.g., Greenstadt & Fredricks 1979; Bavassano Cattaneo et al. 2000). Quasi-perpendicular shocks are characterized by a sharp increase in the magnetic field strength, but quasi-parallel shocks are often more turbulent, with shock ramps containing large-amplitude waves that spread upstream and downstream.

The recent crossing of the termination shock (TS) by *Voyager 1* (*V1*; Burlaga et al. 2005; Decker et al. 2005; Gurnett & Kurth 2005; Stone et al. 2005) provides us with an opportunity to study shocks and shock-induced waves in the heliosheath. The sharp increase in the magnetic field strength across the TS and the downstream magnetic field configuration suggest that the TS is quasi-perpendicular (Burlaga et al. 2005). As in planetary magnetosheaths downstream of a quasi-perpendicular bow shock, the heliosheath shows compressive magnetic fluctuations in the form of magnetic holes (Burlaga et al. 2006a, 2006b).

We propose a theoretical explanation for the temperature anisotropies and associated instabilities induced at a shock. Based on the theoretical analysis, we show that the magnetic holes observed in the heliosheath could be mirror-mode fluctuations. The present results also provide us with a prototype for understanding shocks in various astrophysical contexts, such as gamma-ray bursts, supernova explosions, and active galactic nuclei.

2. THEORY

An anisotropic ion distribution requires the use of a pressure tensor in the magnetohydrodynamic (MHD) equations. Observations show that the shock structure and dynamics depend on the shock geometry and upstream M_{A1} and β_1, so we examine the temperature anisotropy $A_2 = T_{\perp 2}/T_{\parallel 2}$ as a function of these parameters, where $T_\perp$ and $T_\parallel$ are the plasma temperature perpendicular and parallel to the magnetic field, respectively. The subscripts 1 and 2 indicate physical parameters upstream and downstream of a shock. Assuming a bi-Maxwellian plasma, we write the jump conditions across a shock as (Hudson 1970)

$$[B_n] = 0, \tag{1}$$

$$[\rho v_n] = 0, \tag{2}$$

$$[v_n \boldsymbol{B}_t - \boldsymbol{v}_t B_n] = 0, \tag{3}$$

$$\left[P_\perp + (P_\parallel - P_\perp)\frac{B_n^2}{B^2} + \frac{B_t^2 - B_n^2}{2\mu_0} + \rho v_n^2\right] = 0, \tag{4}$$

$$\left[\frac{B_n \boldsymbol{B}_t}{\mu_0}\left(\frac{P_\parallel - P_\perp}{B^2/\mu_0} - 1\right) + \rho v_n \boldsymbol{v}_t\right] = 0, \tag{5}$$

$$\left[\rho v_n\left(\frac{2P_\perp}{\rho} + \frac{P_\parallel}{2\rho} + \frac{v^2}{2} + \frac{B_t^2}{\mu_0 \rho}\right) + \frac{B_n^2 v_n}{B^2}(P_\parallel - P_\perp) - \frac{(\boldsymbol{B}_t \cdot \boldsymbol{v}_t)B_n}{\mu_0}\left(1 - \frac{P_\parallel - P_\perp}{B^2/\mu_0}\right)\right] = 0, \tag{6}$$

[1] Kavli Institute for Astrophysics and Space Research, Massachusetts Institute of Technology, Cambridge, MA 02139; liuxying@mit.edu.

[2] State Key Laboratory of Space Weather, Chinese Academy of Sciences, Beijing 100080, China.

where μ_0 is the permeability of a vacuum, ρ is the plasma density, and $\boldsymbol{v}$ and $\boldsymbol{B}$ are the plasma velocity and magnetic field, respectively, with subscripts t and n denoting the tangential and normal components with respect to the shock surface. The velocity is measured in the shock frame. The square brackets indicate the difference between the preshock (1) and postshock (2) states. The perpendicular and parallel plasma pressures are defined as $P_\perp = \rho k_B T_\perp / m_p$ and $P_\parallel = \rho k_B T_\parallel / m_p$, where k_B and m_p represent the Boltzmann constant and proton mass, respectively. For simplicity, we assume that the bulk velocity is parallel to the shock normal. The components of the magnetic field upstream of the shock are given by $B_{n1} = B_1 \cos\theta_{Bn}$ and $B_{t1} = B_1 \sin\theta_{Bn}$. Different forms of the solutions to these equations have been derived based on various assumptions (Chao et al. 1995; Erkaev et al. 2000). The focus of the present analysis is to investigate under what conditions the shocked plasma is unstable to the thermal anisotropy instabilities.

The thermal anisotropy serves a free energy source that can feed magnetic fluctuations when it exceeds certain threshold conditions. The thresholds can be expressed as $A = 1 - 2/\beta_\parallel$ for the fire-hose instability (Parker 1958), the lower bound of the temperature anisotropy, and $A = 1 + 1/\beta_\perp$ for the mirror-mode instability (Chandrasekhar et al. 1958; Hasegawa 1969), the upper bound. The ion-cyclotron instability, competing with the mirror mode, has the onset condition $A = 1 + 0.64/\beta_\parallel^{0.41}$ (Gary et al. 1997). Here the perpendicular and parallel plasma β's are defined as $\beta_\perp = P_\perp/(B^2/2\mu_0)$ and $\beta_\parallel = P_\parallel/(B^2/2\mu_0)$.

For a perpendicular shock, equations (2) and (3) give the shock strength

$$r_s = \frac{\rho_2}{\rho_1} = \frac{v_1}{v_2} = \frac{B_2}{B_1}. \tag{7}$$

The temperature anisotropy A_2 can be obtained from equations (4), (5), and (6),

$$A_2 = \left[\frac{3A_1\beta_1}{2A_1+1} + 2M_{A1}^2\left(1-\frac{1}{r_s}\right) + 1 - r_s^2\right] \times \left[\frac{3A_1\beta_1}{2A_1+1}\left(4r_s - 4 + \frac{r_s}{A_1}\right) + 2M_{A1}^2\left(r_s + \frac{3}{r_s} - 4\right) + 4(r_s-1)\right]^{-1}, \tag{8}$$

where $\beta = (2P_\perp + P_\parallel)/(3B^2/2\mu_0)$. To compare with the thresholds, we derive $\beta_{\perp 2}$ from equation (4) as

$$\beta_{\perp 2} = \frac{3A_1\beta_1}{(2A_1+1)r_s^2} + \frac{2M_{A1}^2}{r_s^2}\left(1-\frac{1}{r_s}\right) - 1 + \frac{1}{r_s^2}. \tag{9}$$

For $2M_{A1}^2 \gg \beta_1$, we have $\beta_{\perp 2} \sim 2M_{A1}^2/r_s^2$, so the shocked plasma would have a high β independent of β_1, consistent with the findings in the magnetosheaths of outer planets (Russell et al. 1990). As can be seen from the mirror-mode threshold, high values of $\beta_{\perp 2}$ favor the onset of the mirror-mode instability; similarly, $A_2 \sim 1/(r_s - 3)$ under the same condition, so $A_2 \geq 1$ since the shock strength cannot be larger than 4, also favoring the mirror-mode onset.

Figure 1 shows the temperature anisotropy A_2 for $r_s = 3$ and $A_1 = 1$ as a function of M_{A1} and β_1. Only values of $0 \leq A_2 \leq 2$ are shown. The entropy, $S = \frac{1}{2}k_B \ln(P_\perp^2 P_\parallel/\rho^5)$, is required to increase across a shock by the second law of thermodynamics; the region that breaks the entropy principle is show as "Forbidden" in Figure 1. The majority of the allowed area has $A_2 \geq 1$, as expected, and is preferentially unstable to the mirror-mode instability. The mirror mode has a lower threshold than the cyclotron mode in this plasma regime, so the temperature anisotropy would be quickly reduced by the mirror mode before the ion-cyclotron mode could develop. The TS with $\beta_1 \simeq 32.8$ and $M_{A1} \simeq 16.3$ (see § 3), indicated by the plus sign, is located slightly above the mirror-mode threshold. Interplanetary and planetary bow shocks have a large variation in M_{A1} and β_1; many of them would also be above the mirror-mode threshold as indicated by the large area with $A_2 \geq 1$. Consequently, mirror-mode instabilities should be a frequent feature downstream of quasi-perpendicular shocks.

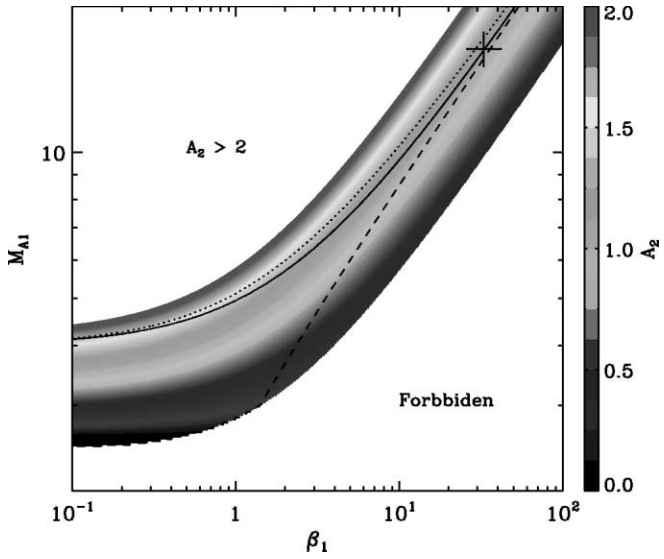

FIG. 1.—Temperature anisotropy downstream of a perpendicular shock with $r_s = 3$ and $A_1 = 1$ as a function of β_1 and M_{A1}. The color shading denotes the values of A_2. The lower region is forbidden for a $r_s = 3$ shock since the entropy does not increase across the shock. Also shown are the thresholds for the mirror-mode (*solid line*), ion-cyclotron (*dotted line*), and fire-hose (*dashed line*) instabilities. Regions above the mirror/ion-cyclotron threshold are unstable to the mirror/ion-cyclotron mode, and regions below the fire-hose onset are unstable to the fire-hose instability. The plus sign marks the TS location. [*See the electronic edition of the Journal for a color version of this figure*.]

For a parallel shock, the magnetic field does not go into the expression of the shock strength. The temperature anisotropy

$$A_2 = \left[\frac{3\beta_1 r_s}{2A_1+1}\left(A_1 + \frac{3}{2} - \frac{3}{2r_s}\right) + M_{A1}^2\left(r_s + \frac{2}{r_s} - 3\right)\right] \times \left[\frac{3\beta_1}{2A_1+1} + 2M_{A1}^2\left(1-\frac{1}{r_s}\right)\right]^{-1}, \tag{10}$$

and the downstream parallel plasma β

$$\beta_{\parallel 2} = \frac{3\beta_1}{2A_1+1} + 2M_{A1}^2\left(1-\frac{1}{r_s}\right). \tag{11}$$

For $2M_{A1}^2 \gg \beta_1$, $\beta_{\parallel 2} \sim 2M_{A1}^2$, which makes the thresholds close to 1, and $A_2 \sim (r_s - 2)/2 \leq 1$, giving favorable conditions for the onset of the fire-hose instability. Figure 2 displays the temperature anisotropy A_2 over various upstream conditions for $r_s = 3$ and $A_1 = 1$. Compared with Figure 1, higher values of M_{A1} at a given β_1 would otherwise lead to smaller A_2. Most of

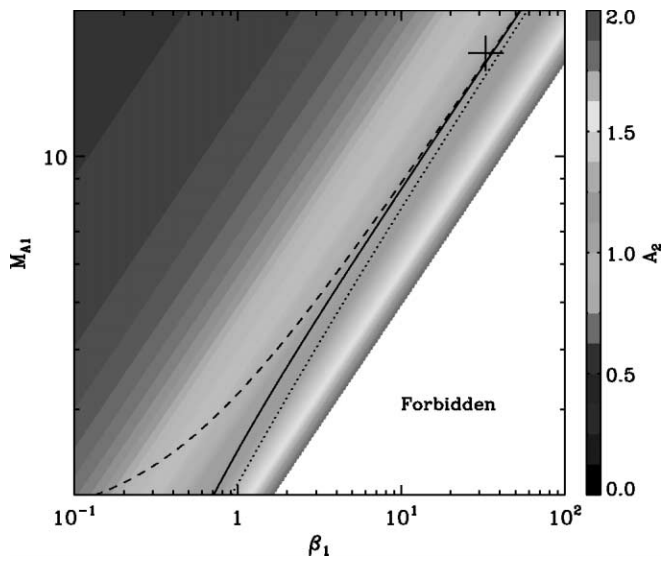

FIG. 2.—Same format as Fig. 1, but for temperature anisotropy downstream of a parallel shock with $r_s = 3$ and $A_1 = 1$ as a function of β_1 and M_{A1}. Regions below the mirror/ion-cyclotron threshold are unstable to the mirror/ion-cyclotron mode, and regions above the fire-hose onset are unstable to the fire-hose instability. [*See the electronic edition of the Journal for a color version of this figure*.]

the area shown has $A_2 \leq 1$, as expected for a quasi-parallel shock, and is unstable to the fire-hose instability. The TS would induce fire-hose instabilities in the downstream plasma if it were quasi-parallel, as indicated by its location in the plot. Many quasi-parallel interplanetary and planetary bow shocks will also give rise to fire-hose instabilities as implied by the large area with $A_2 \leq 1$.

Observations show that a quasi-parallel bow shock becomes unsteady as the Alfvén Mach number M_{A1} exceeds ~3 for $\beta_1 \sim 0.5$ (Greenstadt & Fredricks 1979) and is often associated with large transverse magnetic fluctuations (Bavassano Cattaneo et al. 2000; Czaykowska et al. 2001). A closer look at Figure 2 gives $A_2 \simeq 0.97$ at $M_{A1} = 2$ for $\beta_1 = 0.5$, a noticeable thermal anisotropy but not large enough to exceed the fire-hose onset; at $M_{A1} = 3$, the thermal anisotropy rises above the fire-hose threshold, generating fire-hose instabilities that will disturb the shock structure. The fire-hose instability arises from the fast MHD mode and produces large-amplitude transverse waves. The results from this simple calculation agree with hybrid simulations (Kan & Swift 1983; Krauss-Varban & Omidi 1991).

3. MAGNETIC FLUCTUATIONS IN THE HELIOSHEATH

V1 crossed the TS on 2004 December 16 (day 351) at 94 AU and is making the first measurements in the heliosheath. The magnetic fluctuations in the heliosheath are characterized by a series of depressions in the field magnitude that have been called magnetic holes (Burlaga et al. 2006a, 2006b). These fluctuations are similar to those observed downstream of quasi-perpendicular interplanetary and planetary bow shocks that have been identified as mirror-mode structures (Kaufmann et al. 1970; Tsurutani et al. 1992; Violante et al. 1995; Bavassano Cattaneo et al. 1998).

The TS is expected to be highly oblique with $\theta_{Bn} \sim 86°$ at *V1*, so we use equations (8) and (9) to determine whether mirror-mode instabilities occur in the heliosheath. MHD simulations give the average preshock plasma density $n_1 \simeq 8 \times 10^{-4}$ cm^{-3}, speed $v_1 \simeq 380$ km s^{-1}, and temperature $T_1 \simeq 5.4 \times 10^5$ K (Whang et al. 2004), which yields $M_{A1} \simeq 16.3$, $\beta_1 \simeq 32.8$ combined with the observed field strength $B_1 \simeq 0.03$ nT. The shock strength r_s is ~3 estimated from the jump in the field magnitude (Burlaga et al. 2005) and from the spectral slope of TS accelerated particles (Stone et al. 2005). The typical thermal anisotropy of the solar wind is $A \sim 0.7$ near the Earth (Liu et al. 2006a). Expansion of the solar wind would further decrease the value of A if the magnetic moment $\mu \sim T_\perp/B$ is invariant; when the thermal anisotropy exceeds the fire-hose threshold, fire-hose instabilities will be induced and will help suppress the growth of the anisotropy. The two competing processes will arrive at a balance close to the threshold, i.e., $A \simeq 1 - 2/\beta_\parallel$, which gives $A_1 \simeq 0.94$. Introduction of pickup ions in the outer heliosphere would not significantly change this value. The newly born pickup ions gyrate about the interplanetary magnetic field, forming a ring-beam distribution; this configuration is unstable to the generation of MHD waves, which scatter the ions quickly toward isotropy (Lee & Ip 1987; Bogdan et al. 1991). We have also shown that A_2 does not depend on A_1 when $2M_{A1}^2 \gg \beta_1$. Substituting the values of M_{A1}, β_1, r_s, and A_1 into equations (8) and (9) gives $A_2 \simeq 1.03$ and $\beta_{\perp 2} \simeq 42.2$. The threshold of the mirror mode is $1 + 1/\beta_{\perp 2} \simeq 1.02$, smaller than the downstream anisotropy. As indicated by Figure 1, even an A_2 slightly larger than 1 can meet the mirror-mode onset at high β_1, so mirror-mode instabilities should be induced in the heliosheath.

For the upstream temperature, we have used the density-weighted average of the pickup ion, solar wind proton and electron temperatures (Whang et al. 2004). However, the result can be shown to be self-consistent. Equation (9) is reduced to $\beta_2 \sim (2M_{A1}^2/r_s^2)(1 - 1/r_s)$ in the TS case, from which we have the downstream temperature $T_2 \sim 2 \times 10^6$ K given the average field magnitude $B_2 \simeq 0.09$ nT and density $n_2 \simeq 0.002$ cm^{-3} from equation (7). Approximating the TS as a hydrodynamic shock because of the high plasma β,

$$\frac{T_2}{T_1} = \frac{[2\gamma M^2 - (\gamma - 1)][(\gamma - 1)M^2 + 2]}{(\gamma + 1)^2 M^2},$$

we obtain $T_1 \sim 5 \times 10^5$ K, consistent with the MHD simulation result. Here $\gamma = 5/3$, and $M \simeq 3$, the shock Mach number estimated from $n_2/n_1 \simeq 3$.

Given the absence of plasma measurements across the TS, it is hard to estimate the uncertainties brought about by the upstream conditions and the shock parameters. A revisit to equations (1)–(6) assuming a 10% error in the upstream conditions and the shock geometry and strength gives $A_2 = 1.03 \pm 0.42$ and a mirror-mode threshold 1.02 ± 0.01. Note that the uncertainty of A_2 is determined largely by the shock strength, since $A_2 \sim 1/(r_s - 3)$ in the case of the TS. If we use $r_s = 2.6^{+0.4}_{-0.2}$ inferred from the particle spectra (Stone et al. 2005) with other parameters fixed, then the temperature anisotropy $A_2 = 1.03$–4.19, so the mirror mode would be more likely to occur. Interestingly, the shock strength cannot be smaller than 2.2 at the present conditions, otherwise A_2 would be negative. It should be emphasized that turbulence induced by the mirror-mode instability would leave the threshold marginally satisfied, so we expect $A_2 = 1.02 \pm 0.01$ in the evolved state.

The mirror-mode instability has a maximum growth rate at a wavevector that is highly oblique to the background magnetic field. The minimum variance direction of the measured magnetic fields has an angle of about 75° with respect to the back-

ground field when magnetic holes are present (Burlaga et al. 2006b). Mirror-mode waves are nonpropagating and appear to be static structures, consistent with the observed magnetic fluctuations with a fairly constant field direction (Burlaga et al. 2006a, 2006b). Mirror-mode waves are also characterized by anticorrelated density and magnetic fluctuations. The density measurements are not available, so we cannot verify the mirror mode from density fluctuations. The density perturbation δn can be estimated from (Hasegawa 1969)

$$\frac{\delta n}{n} = -\left(\frac{T_\perp}{T_\parallel} - 1\right)\frac{\delta B}{B},$$

where δB is the perturbation in the field strength. The fluctuation amplitude $\delta B/B$ is ~0.4–0.9 in the heliosheath, which results in $\delta n/n \sim 0.01$–0.03, too small to be resolved by future *V2* observations.

The nonlinear evolution of mirror-mode instabilities would also generate holes in the background field strength (Kivelson & Southwood 1996). The magnetic holes in the heliosheath are of a similar size (in units of the proton gyroradius) to those in planetary magnetosheaths that are predominately produced by mirror-mode waves (Kaufmann et al. 1970; Bavassano Cattaneo et al. 1998; Burlaga et al. 2006b). Magnetic holes in planetary magnetosheaths have also been explained as slow-mode solitons based on Hall-MHD theory (Stasiewicz 2004). The plasma β in the heliosheath is ~40 as estimated above; in this case, the ion Larmor radius is much larger than the ion inertial length, so the Hall-MHD theory breaks down (Pokhotelov et al. 2005).

Deep in the heliosheath, magnetic field lines may be draped and compressed against the heliopause if there is no significant reconnection between the solar wind and interstellar fields. Analogous to planetary magnetosheaths, the plasma would be squeezed and would flow along the draped field lines, leading to a plasma depletion layer close to the heliopause. The plasma β is reduced in this layer, so the mirror-mode instability may be inhibited and ion-cyclotron waves may be generated. Damping of these waves would suppress the thermal anisotropy and would heat the plasma (Liu et al. 2006a).

4. SUMMARY

A simple calculation based on temperature anisotropy instabilities explains a variety of observations associated with interplanetary and planetary bow shocks. A shock modifies the velocity distribution of particles at its surface, producing instabilities downstream of the shock that give rise to different types of waves. The calculation also predicts that mirror-mode waves form downstream of the TS, which is consistent with the observed magnetic fluctuations. The present results provide a substantial basis for shock-induced anisotropies that act as an energy source for plasma heating in various space and astrophysical environments.

The research was supported by NASA contract 959203 from JPL to MIT, NASA grant NAG5-11623, and the NASA Planetary Atmospheres and Outer Planets Programs. This work was also supported by the CAS International Partnership Program for Creative Research Teams.

REFERENCES

Anderson, B. J., Fuselier, S. A., Gary, S. P., & Denton, R. E. 1994, J. Geophys. Res., 99, 5877
Bavassano Cattaneo, M. B., Basile, C., Moreno, G., & Richardson, J. D. 1998, J. Geophys. Res., 103, 11961
———. 2000, J. Geophys. Res., 105, 23141
Bogdan, T. J., Lee, M. A., & Schneider, P. 1991, J. Geophys. Res., 96, 161
Burlaga, L. F., Ness, N. F., & Acuña, M. H. 2006a, ApJ, 642, 584
———. 2006b, Geophys. Res. Lett., 33, L21106, DOI: 10.1029/2006GL027276
Burlaga, L. F., et al. 2005, Science, 309, 2027
Chandrasekhar, S. A., Kaufman, A. N., & Watson, K. M. 1958, Proc. R. Soc. London A, 245, 435
Chao, J. K., Zhang, X. X., & Song, P. 1995, Geophys. Res. Lett., 22, 2409
Czaykowska, A., Bauer, T. M., Treumann, R. A., & Baumjohann, W. 2001, Ann. Geophys., 19, 275
Decker, R. B., et al. 2005, Science, 309, 2020
Erkaev, N. V., Vogl, D. F., & Biernat, H. K. 2000, J. Plasma Phys., 64, 561
Gary, S. P., Wang, J., Winske, D., & Fuselier, S. A. 1997, J. Geophys. Res., 102, 27159
Greenstadt, E. W., & Fredricks, R. W. 1979, in Solar System Plasma Physics, ed. L. J. Lanzerotti, C. F. Kennel, & E. N. Parker (Amsterdam: North-Holland), 3
Gurnett, D. A., & Kurth, W. S. 2005, Science, 309, 2025
Hasegawa, A. 1969, Phys. Fluids, 12, 2642
Hudson, P. D. 1970, Planet. Space Sci., 18, 1611
Kan, J. R., & Swift, D. W. 1983, J. Geophys. Res., 88, 6919
Kaufmann, R. L., Horng, J.-T., & Wolfe, A. 1970, J. Geophys. Res., 75, 4666
Kivelson, M. G., & Southwood, D. J. 1996, J. Geophys. Res., 101, 17365
Krauss-Varban, D., & Omidi, N. 1991, J. Geophys. Res., 96, 17715
Lee, M. A., & Ip, W.-H. 1987, J. Geophys. Res., 92, 11041
Liu, Y., Richardson, J. D., Belcher, J. W., Kasper, J. C., & Elliott, H. A. 2006a, J. Geophys. Res., 111, A01102, DOI: 10.1029/2005JA011329
Liu, Y., Richardson, J. D., Belcher, J. W., Kasper, J. C., & Skoug, R. M. 2006b, J. Geophys. Res., 111, A09108, DOI: 10.1029/2006JA011723
Parker, E. N. 1958, Phys. Rev., 109, 1874
Pokhotelov, O. A., Balikhin, M. A., Sagdeev, R. Z., & Treumann, R. A. 2005, Phys. Rev. Lett., 95, 129501
Russell, C. T., Lepping, R. P., & Smith, C. W. 1990, J. Geophys. Res., 95, 2273
Stasiewicz, K. 2004, Geophys. Res. Lett., 31, L21804
Stone, E. C., et al. 2005, Science, 309, 2017
Tsurutani, B. T., Southwood, D. J., Smith, E. J., & Balogh, A. 1992, Geophys. Res. Lett., 19, 1267
Violante, L., Bavassano Cattaneo, M. B., Moreno, G., & Richardson, J. D. 1995, J. Geophys. Res., 100, 12047
Whang, Y. C., Burlaga, L. F., Wang, Y.-M., & Sheeley, N. R. 2004, Geophys. Res. Lett., 31, 3805